

**Original citation:**

Patchett, Ruth, Knighton, Richard C., Mattock, James D, Vargas, Alfredo and Chaplin, Adrian B.. (2017) Potassium binding adjacent to cationic transition metal fragments : unusual heterobimetallic adducts of a calix[4]arene-based thione ligand. *Inorganic Chemistry*, 56 (22). pp. 14345-14350.

**Permanent WRAP URL:**

<http://wrap.warwick.ac.uk/93598>

**Copyright and reuse:**

The Warwick Research Archive Portal (WRAP) makes this work of researchers of the University of Warwick available open access under the following conditions.

This article is made available under the Creative Commons Attribution 4.0 International license (CC BY 4.0) and may be reused according to the conditions of the license. For more details see: <http://creativecommons.org/licenses/by/4.0/>

**A note on versions:**

The version presented in WRAP is the published version, or, version of record, and may be cited as it appears here.

For more information, please contact the WRAP Team at: [wrap@warwick.ac.uk](mailto:wrap@warwick.ac.uk)

## Potassium Binding Adjacent to Cationic Transition-Metal Fragments: Unusual Heterobimetallic Adducts of a Calix[4]arene-Based Thione Ligand

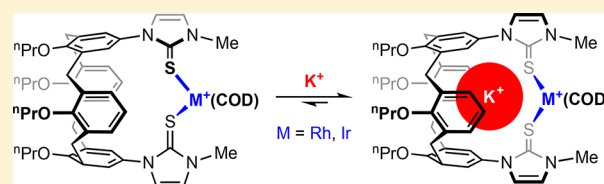
Ruth Patchett,<sup>†</sup> Richard C. Knighton,<sup>†,§</sup> James D. Mattock,<sup>‡,§</sup> Alfredo Vargas,<sup>‡</sup> and Adrian B. Chaplin<sup>\*,†,§</sup>

<sup>†</sup>Department of Chemistry, University of Warwick, Gibbet Hill Road, Coventry CV4 7AL, U.K.

<sup>‡</sup>Department of Chemistry, School of Life Sciences, University of Sussex, Brighton BN1 9QJ, U.K.

### Supporting Information

**ABSTRACT:** The synthesis of cationic rhodium and iridium complexes of a bis(imidazole-2-thione)-functionalized calix[4]-arene ligand and their surprising capacity for potassium binding are described. In both cases, uptake of the alkali metal into the calix[4]arene cavity occurs despite adverse electrostatic interactions associated with close proximity to the transition-metal fragment [ $\text{Rh}^+ \cdots \text{K}^+ = 3.715(1) \text{ \AA}$ ;  $\text{Ir}^+ \cdots \text{K}^+ = 3.690(1) \text{ \AA}$ ]. The formation and constituent bonding of these unusual heterobimetallic adducts have been interrogated through extensive solution and solid-state characterization, examination of the host–guest chemistry of the ligand and its upper-rim unfunctionalized calix[4]arene analogue, and use of density functional theory based energy decomposition analysis.



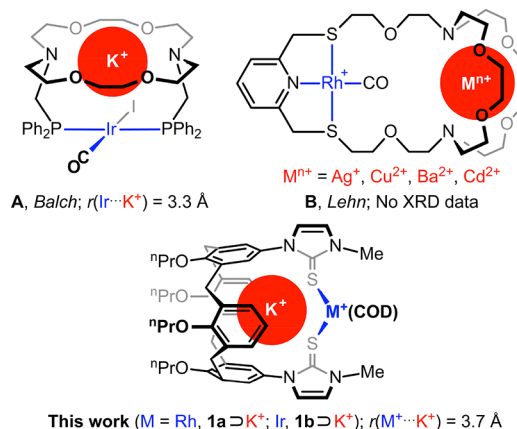
## INTRODUCTION

Electrostatic forces between ions are the strongest noncovalent bonding interactions encountered in supramolecular chemistry. Correspondingly, the attraction between oppositely charged components features widely throughout the host–guest chemistry of biological and synthetic systems.<sup>1</sup> Conversely, repulsion between identically charged host and guest molecules is significantly destabilizing, and unsurprisingly well-defined supramolecular complexes featuring such unfavorable interactions are rare.<sup>2,3</sup>

As part of our ongoing work exploring the coordination chemistry of calix[4]arene-based ligands,<sup>4</sup> we serendipitously discovered that cationic rhodium and iridium complexes **1**, bearing bis(imidazole-2-thione)-functionalized calix[4]arene ligand **2**, show significant uptake of potassium cations (Chart 1). Although alkali-metal binding by calix[4]arenes is well documented, it is typically buttressed by the presence of alkoxide, poly(ether), or carboxyl appendages.<sup>5</sup> In the case of **1**, inclusion of potassium is remarkable for the adverse Coulombic repulsion associated with close proximity of a cationic metal fragment to the binding site ( $M^+ \cdots K^+ = 3.7 \text{ \AA}$ , where  $M = \text{Rh}, \text{Ir}$ ). Indeed, to the best of our knowledge, the nearest well-defined precedent for the host–guest chemistry observed for **1** is neutral iridium host **A** described by Balch ( $\text{Ir} \cdots \text{K}^+ = 3.3 \text{ \AA}$ ; Chart 1).<sup>6</sup> Polycyclic rhodium systems typified by **B** and reported by Carroy and Lehn are conceptually similar, although in this case, the guest cations are held significantly more remote from the rhodium center.<sup>3</sup>

Herein we describe the synthesis of **1** and isolation of the corresponding potassium adducts  $1 \supset \text{K}^+$ . All have been fully characterized in solution and the solid-state using X-ray diffraction. In order to probe the interplay between the

Chart 1. Potassium Binding by Rhodium and Iridium-Based Hosts (COD = 1,5-Cyclooctadiene)



interactions associated with the potassium cation binding, the host–guest chemistry of **1** is contrasted with that of bis(imidazole-2-thione) **2** and calix[4]arene **3** (Figure 1). Density functional theory (DFT) calculations have also been used to help gain insight into the formation of these curious binuclear complexes.

## RESULTS AND DISCUSSION

**Synthesis and Host–Guest Chemistry of Calix[4]-arenes **2** and **3**.** The new bis(imidazole-2-thione) ligand **2** was prepared through reaction of the corresponding bis-

Received: September 25, 2017

Published: November 2, 2017

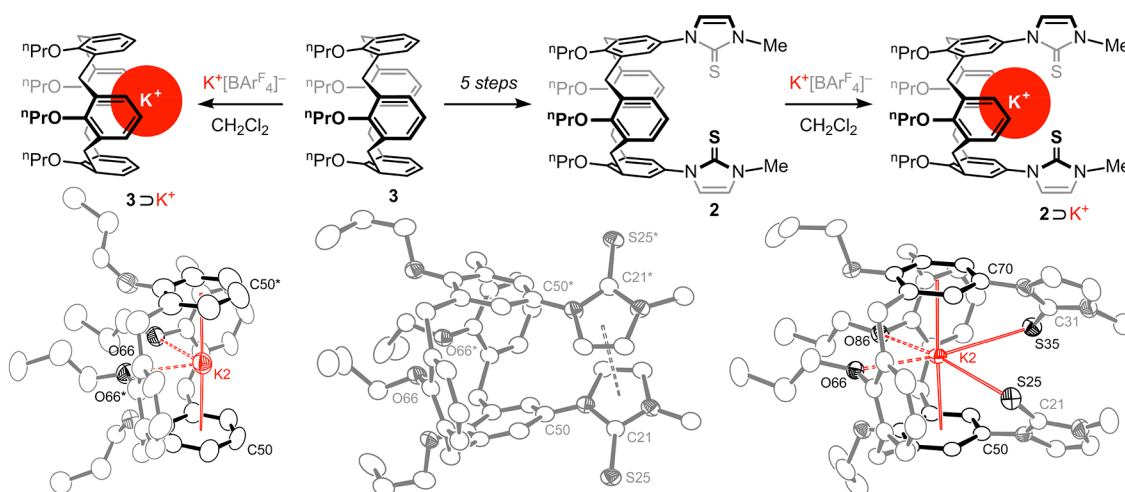


**Figure 1.** Potassium binding of **2** and **3**. Solid-state structures of **2**,  $2\text{K}^+$ , and  $3\text{K}^+$  (ellipsoids drawn at 30%, 50%, and 30% probability, respectively; symmetry equivalent atoms indicated by asterisks; minor distorted components in  $3\text{K}^+$  omitted).  $[\text{BAr}^{\text{F}}_4]^-$  counteranions omitted from all structures. Selected bond lengths (Å): **2**, S25–C21, 1.687(6); Cnt(N20–C24)–Cnt(N20\*–C24\*), 3.46(1); C50–C50\*, 4.24(1) (\* =  $x$ ,  $1 - y$ ,  $1/2 - z$ );  $2\text{K}^+$ , K2–S25, 3.4019(7); K2–S35, 3.4102(6); K2–Cnt(C50–S5), 2.712(2); K2–Cnt(C70–75), 2.711(2); K2–O66, 2.845(1); K2–O86, 2.807(2); S25–C21, 1.679(2); S35–C31, 1.681(2); C50–C70, 5.306(3);  $3\text{K}^+$ : K2–Cnt(C50–S5), 2.790(9); K2–O66, 2.830(5); C50–C50\*, 5.71(2) (\* =  $3 - x$ ,  $3/2 - y$ ,  $z$ ).

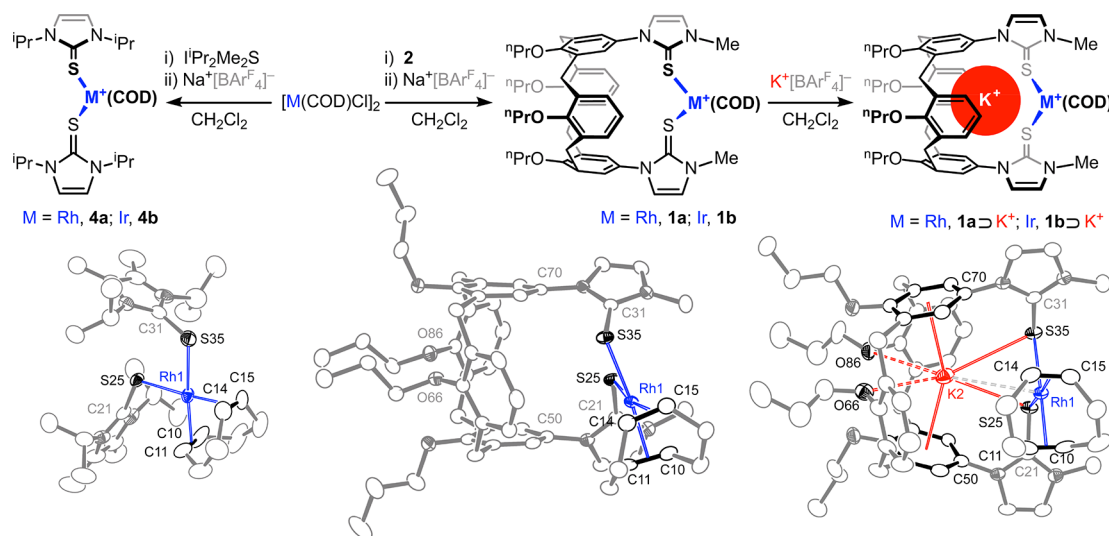


**Figure 2.** Preparation of **1**,  $1\text{aK}^+$ , and **4**. Solid-state structures of **1a**,  $1\text{aK}^+$ , and **4a** (ellipsoids drawn at 50% probability; minor distorted components omitted).  $[\text{BAr}^{\text{F}}_4]^-$  counteranions omitted from all structures. Selected bond lengths (Å) and angles (deg): **1a**, Rh1–Cnt(C10,11), 2.030(2); Rh1–Cnt(C14,15), 2.015(2); Rh1–S25, 2.3515(5); Rh1–S35, 2.3756(5); C10–C11, 1.386(3); C14–C15, 1.394(3); S25–C21, 1.705(2); S35–C31, 1.720(2); S25–Rh1–S35, 83.81(2); C50–C70, 5.387(3); **1b**, Ir1–Cnt(C10,11), 2.017(3); Ir1–Cnt(C14,15), 2.005(3); Ir1–S25, 2.3390(8); Ir1–S35, 2.3604(8); C10–C11, 1.407(5); C14–C15, 1.422(5); S25–C21, 1.709(3); S35–C31, 1.732(3); S25–Ir1–S35, 84.40(3); C50–C70, 5.385(5);  $1\text{aK}^+$ , Rh1–K2, 3.715(1); Rh1–Cnt(C10,11), 2.023(4); Rh1–Cnt(C14,15), 2.029(4); Rh1–S25, 2.366(1); Rh1–S35, 2.3850(9); C10–C11, 1.387(7); C14–C15, 1.386(6); S25–C21, 1.716(4); S35–C31, 1.718(4); S25–Rh1–S35, 77.99(3); K2–S25, 3.472(1); K2–S35, 3.585(2); K2–Cnt(C50–S5), 3.084(4); K2–Cnt(C70–75), 3.078(4); K2–O66, 3.149(3); K2–O86, 3.534(3); C50–C70, 6.709(5);  $1\text{bK}^+$ , Ir1–K2, 3.690(1); Ir1–Cnt(C10,11), 2.015(5); Ir1–Cnt(C14,15), 2.016(5); Ir1–S25, 2.352(1); Ir1–S35, 2.364(1); C10–C11, 1.395(9); C14–C15, 1.381(8); S25–C21, 1.720(5); S35–C31, 1.729(5); S25–Ir1–S35, 78.80(4); K2–S25, 3.521(2); K2–S35, 3.632(2); K2–Cnt(C50–S5), 3.068(5); K2–Cnt(C70–75), 3.065(5); K2–O66, 3.087(4); K2–O86, 3.514(4); C50–C70, 6.691(7); **4a**, Rh1–Cnt(C10,11), 2.010(3); Rh1–Cnt(C14,15), 2.020(3); Rh1–S25, 2.3706(6); Rh1–S35, 2.3671(7); C10–C11, 1.380(5); C14–C15, 1.380(5); S25–C21, 1.727(3); S35–C31, 1.729(3); S25–Rh1–S35, 89.06(2); **4b**, Ir1–Cnt(C10,11), 1.994(4); Ir1–Cnt(C14,15), 2.005(3); Ir1–S25, 2.3496(8); Ir1–S35, 2.3459(9); C10–C11, 1.396(6); C14–C15, 1.403(5); S25–C21, 1.728(3); S35–C31, 1.732(3); S25–Ir1–S35, 89.50(3).

(imidazolium) salt<sup>4</sup> with sulfur in the presence of weak base (72% isolated yield).<sup>7</sup> The solid-state structure of **2** is notable for  $\pi$ -stacking between the imidazole-2-thione moieties [Cnt–Cnt = 3.46(1) Å], which enforces a pronounced pinched cone conformation of the calix[4]arene scaffold and confers overall  $C_2$  symmetry (Figure 1). Although retention of the  $\pi$ -stacking interaction is not apparent in  $\text{CD}_2\text{Cl}_2$  solution at 298 K by  $^1\text{H}$

NMR spectroscopy (600 MHz;  $C_{2v}$  symmetry), the onset of signal decoalescence was observed upon cooling to 200 K.

Mixing **2** with  $\text{K}[\text{BAr}^{\text{F}}_4]$  [ $\text{Ar}^{\text{F}} = 3,5\text{-(CF}_3)_2\text{C}_6\text{H}_3$ ]<sup>8</sup> in anhydrous  $\text{CD}_2\text{Cl}_2$  resulted in dissolution of the otherwise insoluble salt and formation of the 1:1 host–guest complex  $2\text{K}^+$  (Figure 1). The system is under slow host–guest exchange on the NMR time scale (298 K, 400 MHz) and

allowed the binding stoichiometry to be unambiguously verified through in situ experiments involving variation of the  $2/\text{K}[\text{BAr}^{\text{F}}_4]$  ratio (see Figure S44). On a preparative scale, the potassium adduct was isolated in high yield by crystallization (86%) and fully characterized. The solid-state structure of  $2\text{OK}^+$  confirms encapsulation of the potassium cation within the calix[4]arene cavity (Figure 1). Supplemented by chelation of the thione ( $\text{S}-\text{K}^+$  ca. 3.41 Å), the opposing aryl imidazole-2-thione units bind potassium [ $\text{Cnt}(\text{Ar}^{\text{S}})-\text{K}^+$  ca. 2.71 Å], in a sandwich-type  $\pi$ -complex arrangement. The adjacent aryl ether units are associated with  $\text{Ar}^{\text{H}}\text{O}\cdots\text{K}^+$  contacts of ca. 2.83 Å. Sharp  $^1\text{H}$  resonances and  $\text{C}_{2v}$  symmetry are observed for  $2\text{OK}^+$  in  $\text{CD}_2\text{Cl}_2$  across a wide temperature range (298–200 K, 600 MHz), indicating that the  $\text{S}-\text{K}^+$  interaction is highly fluxional in nature.

In a similar manner, formation of a 1:1 potassium adduct of upper-rim-unfunctionalized calix[4]arene **3** was established in  $\text{CD}_2\text{Cl}_2$  solution (slow host–guest exchange at 298 K, 400 MHz) and crystalline  $3\text{OK}^+$  was subsequently obtained in 80% isolated yield. A core structure comparable to  $2\text{OK}^+$  is observed in the solid state, exemplified by alternating arene– $\pi$  interactions [2.790(9) Å] and short lower-rim oxygen contacts [2.830(5) Å] with the alkali-metal cation (Figure 1). In  $\text{CD}_2\text{Cl}_2$  solution, potassium binding results in reduced structural dynamics of the otherwise flexible calix[4]arene scaffold on the  $^1\text{H}$  NMR time scale (600 MHz): most notably, the slow exchange regime is reached at 200 K for  $3\text{OK}^+$  ( $\text{C}_{2v}$ ) but not for **3** ( $\text{C}_{4v}$ ).

To help gauge the energetic importance of thione coordination in the formation of  $2\text{OK}^+$ , a competition experiment was carried out involving the reaction between **2** and  $3\text{OK}^+$  in  $\text{CD}_2\text{Cl}_2$  (eq 1). The resulting dynamic equilibrium showed selective binding of potassium by **2**, but the transfer of potassium from  $3\text{OK}^+$  is only weakly exergonic ( $\Delta G_{298\text{ K}} = -8.4\text{ kJ}\cdot\text{mol}^{-1}$ ).<sup>9</sup> Together the combined solution data suggest that the potassium cation is primarily bound through the calix[4]arene scaffold in  $2\text{OK}^+$ , with comparatively weaker  $\text{S}-\text{K}^+$  interactions. Consistent with this reasoning, 1,3-diisopropyl-4,5-dimethylimidazole-2-thione ( $\text{IPr}_2\text{Me}_2\text{S}$ )<sup>10</sup> does not form a potassium complex upon standing in a suspension of  $\text{K}[\text{BAr}^{\text{F}}_4]$  in  $\text{CD}_2\text{Cl}_2$  at 298 K.<sup>11</sup>

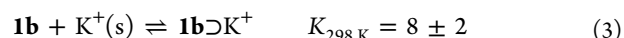
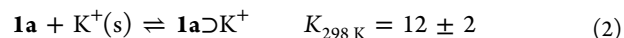


Reactions of  $2\text{OK}^+$  and  $3\text{OK}^+$  with 18-crown-6 resulted in quantitative extraction of potassium from both of the calix[4]arene hosts. Likewise, competition experiments involving [18-crown-6OK][ $\text{BAr}^{\text{F}}_4$ ] [see the Supporting Information (SI) for preparation and solid-state structure;  $\text{O}-\text{K}^+$  ca. 2.77 Å] and **2** or **3** showed no appreciable potassium uptake by the calix[4]arenes. Together these data indicate a relatively low absolute magnitude for the potassium cation binding by **2** and **3** and highlight the importance of employing weakly coordinating solvent and anion in the formation of  $2\text{OK}^+$  and  $3\text{OK}^+$ .

**Synthesis and Host–Guest Chemistry of Rhodium and Iridium Complexes 1.** Cationic rhodium and iridium complexes  $[\text{M}(\text{2})(\text{COD})][\text{BAr}^{\text{F}}_4]$  ( $\text{M} = \text{Rh}$ , **1a**;  $\text{M} = \text{Ir}$ , **1b**) were prepared by reaction of  $[\text{M}(\text{COD})\text{Cl}]_2$ <sup>12</sup> with **2** in  $\text{CH}_2\text{Cl}_2$ , followed by halide abstraction, and isolated in moderate yields (**1a**, 64%; **1b**, 68%; Figure 2). The formation of **1** were fully corroborated using a combination of NMR spectroscopy, electrospray ionization mass spectrometry (ESI-MS), combustion analysis, and X-ray diffraction. Coordination of **2** is associated with a significant upfield shift of the  $\text{C}=\text{S}$

resonance (**1a**,  $\delta$  156.4; **1b**,  $\delta$  154.5; **2**,  $\delta$  163.4) and adoption of  $\text{C}_s$  symmetry in  $\text{CD}_2\text{Cl}_2$  solution at 298 K (600 MHz). The solid-state structures show that the  $\{\text{M}(\text{COD})\}^+$  fragments are projected to one side of the calix[4]arene cavity through asymmetrical cis coordination of the imidazole-2-thione donors, one synperiplanar ( $\text{S2S}$ ) and the other antiperiplanar ( $\text{S3S}$ ) about the  $\text{M}-\text{S}$  vectors, conferring overall  $\text{C}_1$  symmetry. Reconciling this structure in solution, gradual cooling from 298 to 200 K resulted in loss of  $\text{C}_s$  symmetry and signal decoalescence in the  $^1\text{H}$  NMR spectra of **1** ( $\Delta G^\ddagger$ :  $\sim 43\text{ kJ}\cdot\text{mol}^{-1}$ , **1a**;  $\sim 48\text{ kJ}\cdot\text{mol}^{-1}$ , **1b**; Figures S4 and S9). Fluxional behavior of this type is well-known for complexes of sulfur-based ligands.<sup>13</sup> Bis(imidazole-2-thione) complexes  $[\text{M}(\text{IPr}_2\text{Me}_2\text{S})_2(\text{COD})][\text{BAr}^{\text{F}}_4]$  ( $\text{M} = \text{Rh}$ , **4a**;  $\text{Ir}$ , **4b**; Figure 2)<sup>14</sup> were prepared for comparison and also adopt asymmetrical *cis*-thione geometries in the solid state but are significantly more structurally dynamic than **1** in solution.

The potassium binding of **1** was systematically investigated through in situ reactions involving varying ratios of  $\text{K}[\text{BAr}^{\text{F}}_4]$  in anhydrous  $\text{CD}_2\text{Cl}_2$  (Figures S40 and S42). Partial uptake of potassium into solution and formation of 1:1 adducts  $1\text{OK}^+$  (slow exchange at 298 K, 400 MHz) was observed (eqs 2 and 3). Association constants determined by integration of  $^1\text{H}$  NMR data are consistent with marginally stronger potassium binding for **1a** ( $12 \pm 2$ ) compared to **1b** ( $8 \pm 2$ ). Analytically pure samples of  $1\text{OK}^+$  were subsequently obtained in low yield by selective crystallization of the dications from solution (ca. 10%). Reestablishment of the equilibrium occurs upon dissolution of isolated  $1\text{OK}^+$  in  $\text{CD}_2\text{Cl}_2$  solution (ca. 24 h) but is sufficiently slow that the potassium adducts can be comprehensively characterized.

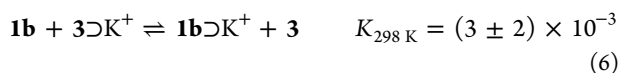
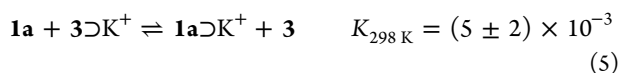


The solid-state structures of  $1\text{OK}^+$  reveal the potassium cation bound within the calix[4]arene cavity in very close proximity to the transition-metal centers:  $\text{Rh}^+\cdots\text{K}^+ = 3.715(1)$  Å;  $\text{Ir}^+\cdots\text{K}^+ = 3.690(1)$  Å (Figure 2). Compared to **1**, the solid-state structures of  $1\text{OK}^+$  are notable for more symmetrical, all-synperiplanar (about the  $\text{M}-\text{S}$  vectors) configurations of the thione donors. The associated  $\text{C}_s$  symmetry is also observed in  $\text{CD}_2\text{Cl}_2$  solution at 298 K. This change in conformational preference was verified in silico (see the SI) and is presumably driven by electrostatic repulsion between the metal atoms. For instance,  $1\text{OK}^+$  are characterized by significantly enlarged proximal  $\text{Cnt}(\text{Ar}^{\text{H}})\cdots\text{M}^+$  distances [ $\text{M}$ :  $\text{Rh}$ , 5.688(5) vs 4.869(2) Å;  $\text{Ir}$ , 5.705(7) vs 4.851(4) Å] and widened calix[4]arene cavity openings, as gauged through the  $(\text{Ar}^{\text{S}})\text{CN}\cdots(\text{Ar}^{\text{S}})\text{CN}$  separations [ $\text{M}$ :  $\text{Rh}$ , 6.709(5) vs 5.387(3) Å;  $\text{Ir}$ , 6.691(7) vs 5.385(5) Å], compared to **1**. Notably, the X-ray-derived metrics associated with the encapsulation of potassium by the calix[4]arene ligand in  $1\text{OK}^+$  are indicative of a weaker interaction compared to those in  $2\text{OK}^+$ , viz.  $\text{Cnt}(\text{Ar}^{\text{S}})-\text{K}^+$  ca. 3.07 vs 2.71 Å,  $\text{S}-\text{K}^+$  ca. 3.55 vs 3.41 Å, and  $\text{Ar}^{\text{H}}\text{O}\cdots\text{K}^+$  ca. 3.12/3.52 vs 2.83 Å.

The partial uptake of potassium into solution observed for **1** and the solid-state metrics of  $1\text{OK}^+$  both imply significantly weaker binding compared to **2**; observations supported by complete retention of potassium by **2** when  $2\text{OK}^+$  was reacted with **1** in competition experiments (eq 4). The associated energetics ( $\Delta G_{298\text{ K}} \sim +22\text{ kJ}\cdot\text{mol}^{-1}$ ) were instead assessed indirectly through competition experiments between **1** and



$3\text{OK}^+$  in  $\text{CD}_2\text{Cl}_2$  (eqs 5 and 6).<sup>9</sup> As for the association constants, the rhodium-based host appears to show a more pronounced capacity for potassium inclusion in these competition experiments  $[(5 \pm 2 \text{ vs } 3 \pm 2) \times 10^{-3}]$ ; however, the large experimental error associated with these values prevents a definitive conclusion to be drawn. Given the weak nature of the  $\text{S}-\text{K}^+$  interaction, it is rather unsurprising that no reactions were detected by  $^1\text{H}$  NMR spectroscopy for control experiments involving **4** and either  $\text{K}[\text{BAr}^{\text{F}}_4]$  (insoluble) or  $3\text{OK}^+$  in  $\text{CD}_2\text{Cl}_2$ . Moreover, quantitative extraction of potassium from  $1\text{OK}^+$  resulted upon addition of 18-crown-6. Thus, although **1** are competent hosts for potassium cation guests, this series of competition experiments unequivocally demonstrate the significant destabilizing effect of the  $\text{M}^+\cdots\text{K}^+$  interaction.



**Computational Analysis of Potassium Binding.** The interactions associated with formation of  $1\text{OK}^+$  were analyzed computationally using a DFT-based energy decomposition analysis (EDA)<sup>15</sup> and compared to those of  $2\text{OK}^+$  and  $3\text{OK}^+$ . Inspection of the deformation densities associated with fragmentation between  $\text{K}^+$  and **1** reveals that the largest charge transfer occurs from the thione donors to potassium (illustrated for  $\mathbf{1aOK}^+$  in Figure 3 and  $\mathbf{1bOK}^+$  in Figure S65;  $\Delta\rho_1-\Delta\rho_3$ ;  $E_\rho = -7.37$  to  $-13.62$   $\text{kJ}\cdot\text{mol}^{-1}$ ). Interestingly, in  $\Delta\rho_3$ , some charge depletion is evident on the transition metal. Significant charge flow also occurs from the aryl ( $\Delta\rho_4-\Delta\rho_6$ ;  $E_\rho = -5.41$  to  $-7.67$   $\text{kJ}\cdot\text{mol}^{-1}$ ) units of the calix[4]arene to potassium but curiously not from the lower-rim oxygen atoms ( $E_\rho < 5$   $\text{kJ}\cdot\text{mol}^{-1}$ ), suggesting that the short  $\text{Ar}^{\text{H}}\text{O}\cdots\text{K}^+$  contacts of ca.

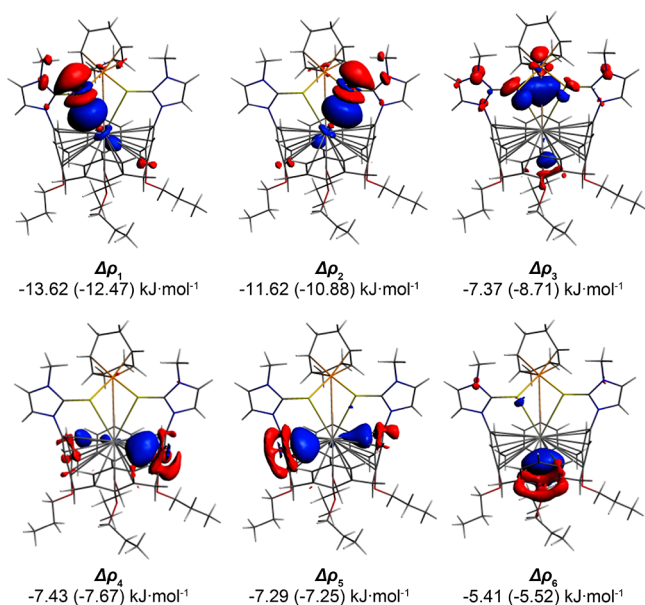


**Figure 3.** Leading ETS-NOCV deformation densities ( $\Delta\rho$ ) and associated eigenvalues for fragmentation between  $\text{K}^+$  and **1a** in  $\mathbf{1aOK}^+$ . Charge flow from red to blue. Energies associated with the equivalent deformation densities in  $\mathbf{1bOK}^+$  are given in parentheses.

$3.12/3.52$  may result from the pinched cone conformation of the calix[4]arene scaffold rather than any meaningful bonding. Equivalent arene- $\pi$  ( $E_\rho = -4.81$  to  $-9.92$   $\text{kJ}\cdot\text{mol}^{-1}$ ) and thione ( $E_\rho = -15.78$  to  $-17.07$   $\text{kJ}\cdot\text{mol}^{-1}$ ) interactions with the potassium cation can be identified in  $2\text{OK}^+$ , with the larger magnitude of these interactions consistent with weaker bonding in  $1\text{OK}^+$  (Figure S66). Even stronger potassium bonding with the aryl units of **3** ( $E_\rho = -7.01$  to  $-12.73$   $\text{kJ}\cdot\text{mol}^{-1}$ ) is evident in  $3\text{OK}^+$  and supplemented in this case by a small degree of charge transfer from the lower-rim oxygen atoms to potassium (Figure S67).

The total bonding energy values derived from EDA ( $E_{\text{Int}}$ ) corroborate the relative potassium binding strengths established experimentally ( $2 > 3 \gg \mathbf{1a} > \mathbf{1b}$ ; Table 1). The similarity of

**Table 1.** EDA of Host–Guest Complexes of Potassium (Energies in  $\text{kJ}\cdot\text{mol}^{-1}$ )

host	$E_{\text{Pauli}}$	$E_{\text{Electro}}$	$E_{\text{Orb Int}}$	$E_{\text{Int}}$
<b>1a</b>	58.46	46.65	−125.37	−20.26
<b>1b</b>	56.09	54.00	−125.41	−15.32
<b>2</b>	78.00	−215.79	−122.70	−260.50
<b>3</b>	91.04	−151.76	−128.93	−189.65

the orbital interaction energies for all of the host–guest adducts (ca.  $-126$   $\text{kJ}\cdot\text{mol}^{-1}$ ) suggests that this bonding component is associated almost exclusively with the calix[4]arene scaffold and marks out electrostatic interactions as the origin of the differences in the binding energy. Correspondingly, it is evident from these data that the ability of **1** to bind potassium, albeit weakly, is only possible because the electrostatic repulsion between potassium and the transition-metal cations (ca.  $+266$   $\text{kJ}\cdot\text{mol}^{-1}$ ) is partially offset by the electrostatic attraction between potassium and the thione donors (ca.  $-64$   $\text{kJ}\cdot\text{mol}^{-1}$ ), and there are significant orbital interactions between the potassium cation and the calix[4]arene cavity. Hirshfeld charges for **1** highlight greater charge differences between the sulfur and rhodium ( $-0.12/+0.19$ ) than between the sulfur and iridium ( $-0.09/+0.07$ ), which presumably accounts for the slightly less unfavorable electrostatic term in the EDA of  $\mathbf{1aOK}^+$ , compared to  $\mathbf{1bOK}^+$ , and correspondingly the marginally different binding affinities of the transition-metal-based hosts.

## SUMMARY AND OUTLOOK

The preparation and host–guest chemistry of cationic rhodium and iridium complexes (**1**) of a new bis(imidazole-2-thione)-functionalized calix[4]arene ligand (**2**) have been presented. Contrary to significantly destabilizing Coulombic repulsion resulting from close proximity to the bound transition metal, these complexes are competent hosts for the 1:1 binding of potassium cations within the central ligand cavity. The formation and constituent bonding of the resulting heterobimetallic adducts ( $1\text{OK}^+$ ) has been interrogated through extensive solution and solid-state characterization, examination of the host–guest chemistry of **2** and its upper-rim-unfunctionalized calix[4]arene analogue **3**, and use of DFT-based EDA. On the basis of this work, the formation of  $1\text{OK}^+$  can be attributed to robust potassium binding by the calix[4]arene scaffold and the ability of the thione donors to partially offset the destabilizing electrostatic repulsion associated with close proximity of the two metal centers ( $\text{M}^+\cdots\text{K}^+ = 3.7$  Å, where  $\text{M} = \text{Rh}, \text{Ir}$ ).

In the context of host–guest chemistry, the formation of  $10K^+$  showcases an unusual confluence of bonding interactions that may inform new approaches for engineering effective molecular receptors, while from an organometallic chemistry perspective, the use of a cavitand-based ligand, such as **2**, to study the unusual coordination chemistry of the late transition metals is a potentially powerful concept. We are particularly interested in exploring the latter as part of our ongoing research at the interface of supramolecular and organometallic chemistry.

## ■ ASSOCIATED CONTENT

### Supporting Information

The Supporting Information is available free of charge on the ACS Publications website at DOI: 10.1021/acs.inorgchem.7b02441.

Full experimental and computational details, NMR and ESI-MS spectra of new compounds, and selected reactions (PDF)

Optimized geometries in .xyz format (XYZ)

### Accession Codes

CCDC 1569667–1569677 contain the supplementary crystallographic data for this paper. These data can be obtained free of charge via [www.ccdc.cam.ac.uk/data\\_request/cif](http://www.ccdc.cam.ac.uk/data_request/cif), or by emailing [data\\_request@ccdc.cam.ac.uk](mailto:data_request@ccdc.cam.ac.uk), or by contacting The Cambridge Crystallographic Data Centre, 12 Union Road, Cambridge CB2 1EZ, UK; fax: +44 1223 336033.

## ■ AUTHOR INFORMATION

### Corresponding Author

\*E-mail: [a.b.chaplin@warwick.ac.uk](mailto:a.b.chaplin@warwick.ac.uk).

### ORCID

Adrian B. Chaplin: 0000-0003-4286-8791

### Author Contributions

<sup>§</sup>These authors contributed equally.

### Notes

The authors declare no competing financial interest.

## ■ ACKNOWLEDGMENTS

We thank the EPSRC (R.P.), Leverhulme Trust (R.C.K.), University of Sussex (A.V.), and Royal Society (A.B.C.) for financial support. Crystallographic data (for all compounds except  $10K^+$ ) and high-resolution mass spectrometry data were collected using instruments purchased through support from Advantage West Midlands and the European Regional Development Fund. Crystallographic data for  $10K^+$  were collected using an instrument that received funding from the ERC under the European Union's Horizon 2020 research and innovation programme (Grant 637313).

## ■ REFERENCES

- (1) Steed, J. W.; Atwood, J. L. *Supramolecular Chemistry*, 2nd ed.; John Wiley & Sons: Sussex, U.K., 2009.
- (2) For representative examples, see: Bourgeois, J.-P.; Fujita, M.; Kawano, M.; Sakamoto, S.; Yamaguchi, K. A Cationic Guest in a 24+ Cationic Host. *J. Am. Chem. Soc.* **2003**, *125*, 9260–9261. McFarland, S. A.; Finney, N. S. Modulating the Efficiency of Ru(II) Luminescence via Ion Binding-Induced Conformational Restriction of Bipyridyl Ligands. *Chem. Commun.* **2003**, 388–389. Beer, P. D.; Dent, S. W. Potassium Cation Induced Switch in Anion Selectivity Exhibited by Heteroditopic Ruthenium(II) and Rhenium(I) Bipyridyl Bis(benzo-15-crown-5) Ion Pair Receptors. *Chem. Commun.* **1998**, 825–826.
- (3) Carroy, A.; Lehn, J.-M. Synthesis and Heterodimetallic Complexes of Lateral Macrobicyclic Cryptands. *J. Chem. Soc., Chem. Commun.* **1986**, 1232–1234.
- (4) Patchett, R.; Chaplin, A. B. Coordination Chemistry of a Calix[4]arene-Based NHC Ligand: Dinuclear Complexes and Comparison to  $[Pr_2Me_2]$ . *Dalton Trans.* **2016**, *45*, 8945–8955.
- (5) For representative examples, see: Li, Y.; Zhao, H.; Mao, X.; Pan, X.; Wu, J. Structures of Potassium Calix[4]arene Crown Ether Inclusion Complexes and Application in Polymerization of *rac*-Lactide. *Dalton Trans.* **2016**, *45*, 9636–9645. Chinta, J. P.; Ramanujam, B.; Rao, C. P. Structural Aspects of the Metal Ion Complexes of the Conjugates of Calix[4]arene: Crystal Structures and Computational Models. *Coord. Chem. Rev.* **2012**, *256*, 2762–2794. Matthews, S. E.; Schmitt, P.; Félix, V.; Drew, M. G. B.; Beer, P. D. Calix[4]tubes: A New Class of Potassium-Selective Ionophore. *J. Am. Chem. Soc.* **2002**, *124*, 1341–1353. Beer, P. D.; Drew, M. G. B.; Gale, P. A.; Leeson, P. B.; Ogden, M. I. Structures of Potassium Encapsulated Within the 1,3-Alternate Conformation of Calix[4]arenes. *J. Chem. Soc., Dalton Trans.* **1994**, 3479–3485. Ikeda, A.; Shinkai, S. On the Origin of High Ionophoricity of 1,3-Alternate Calix[4]arenes:  $\pi$ -Donor Participation in Complexation of Cations and Evidence for Metal-Tunneling Through the Calix[4]arene Cavity. *J. Am. Chem. Soc.* **1994**, *116*, 3102–3110. Iwamoto, K.; Shinkai, S. Synthesis and Ion Selectivity of All Conformational Isomers of Tetrakis[(ethoxycarbonyl)methoxy]-calix[4]arene. *J. Org. Chem.* **1992**, *57*, 7066–7073. Harrowfield, J. M.; Ogden, M. I.; Richmond, W. R.; White, A. H. Calixarene-Cupped Caesium: A Coordination Conundrum? *J. Chem. Soc., Chem. Commun.* **1991**, 1159–1161. Ghidini, E.; Uguzzoli, F.; Ungaro, R.; Harkema, S.; Abu El-Fadl, A.; Reinhoudt, D. N. Complexation of Alkali Metal Cations by Conformationally Rigid, Stereoisomeric Calix[4]arene Crown Ethers: A Quantitative Evaluation of Preorganization. *J. Am. Chem. Soc.* **1990**, *112*, 6979–6985.
- (6) Balch, A. L.; Neve, F.; Olmstead, M. M. Assessing the Effects of Metal Ion Proximity on a *trans*-Ir(CO)Cl(phosphine)<sub>2</sub> Unit. Structural Studies of Potassium(I), Tin(II), and Lead(II) Complexes of (crown-P<sub>2</sub>)Ir(CO)Cl. *Inorg. Chem.* **1991**, *30*, 3395–3402.
- (7) For previous examples of this synthetic methodology, see: Tyson, G. E.; Tokmic, K.; Oian, C. S.; Rabinovich, D.; Valle, H. U.; Hollis, T. K.; Kelly, J. T.; Cuellar, K. A.; McNamara, L. E.; Hammer, N. I.; Webster, C. E.; Oliver, A. G.; Zhang, M. Synthesis, Characterization, Photophysical Properties, and Catalytic Activity of an SCS Bis(N-heterocyclic thione) (SCS-NHT) Pd Pincer Complex. *Dalton Trans.* **2015**, *44*, 14475–14482. Williams, D. J.; Vanderveer, D.; Jones, R. L.; Menaldino, D. S. Main Group Metal Halide Complexes with Sterically Hindered Thioureas XI. Complexes of Antimony(III) and Bismuth(III) Chlorides with a New Bidentate Thiourea – 1,1'-Methylenebis-(3-methyl-2H-imidazole-2-thione). *Inorg. Chim. Acta* **1989**, *165*, 173–178.
- (8) Buschmann, W. E.; Miller, J. S.; Bowman-James, K.; Miller, C. N. Synthesis of  $[M^{II}(NCMe)_6]^{2+}$  (M = V, Cr, Mn, Fe, Co, Ni) Salts of Tetra[3,5-bis(trifluoromethyl)phenyl]borate. *Inorg. Synth.* **2002**, *33*, 83–91.
- (9) These data are supported in silico, although we are reluctant to place too large an emphasis on thermodynamic values calculated in this manner. See the SI for calculated data and details.
- (10) Kuhn, N.; Kratz, T. Synthesis of Imidazol-2-ylidenes by Reduction of Imidazole-2-(3H)-thiones. *Synthesis* **1993**, *1993*, 561–562.
- (11) Formation of  $[I^+Pr_2Me_2S/CH_2Cl][Bar^F_4]$  via oxidative addition of  $CH_2Cl_2$  to the thione does, however, occur upon extended heating. See the SI for full details, including solid-state structure.
- (12) Giordano, G.; Crabtree, R. H.; Heintz, R. M.; Forster, D.; Morris, D. E. Di- $\mu$ -chloro-bis( $\eta^4$ -1,5-cyclooctadiene)-dirhodium(I). *Inorg. Synth.* **1990**, *28*, 88–90. Herde, J. L.; Lambert, J. C.; Senoff, C. V.; Cushing, M. A. Cyclooctene and 1,5-Cyclooctadiene Complexes of Iridium(I). *Inorg. Synth.* **2007**, *15*, 18–20.
- (13) Abel, E. W.; Bhargava, S. K.; Orrell, K. G. The Stereodynamics of Metal Complexes of Sulfur-, Selenium-, and Tellurium-Containing

Ligands. In *Progress in Inorganic Chemistry*; John Wiley & Sons, Inc.: Hoboken, NJ, 1984; Vol. 32, pp 1–118.

(14) The tetrafluoroborate analogue of **4a** has been previously reported: Neveling, A.; Julius, G. R.; Cronje, S.; Esterhuysen, C.; Raubenheimer, H. G. Thione Complexes of Rh(I): A First Comparison with the Bonding and Catalytic Activity of Related Carbene and Imine Compounds. *Dalton Trans.* **2005**, 181–192.

(15) A brief overview of the EDA method is provided in the [SI](#).